GENOMIC EVOLUTION

3D genomics across the tree of life reveals condensin II as a determinant of architecture type

Claire Hoencamp[1]†, Olga Dudchenko[2,3,4]†, Ahmed M. O. Elbatsh[1]†‡, Sumitabha Brahmachari[4]†, Jonne A. Raaijmakers[5]§, Tom van Schaik[6]§, Ángela Sedeño Cacciatore[1]§, Vinícius G. Contessoto[4,7]§, Roy G. H. P. van Heesbeen[5]§¶, Bram van den Broek[8], Aditya N. Mhaskar[1]#, Hans Teunissen[6], Brian Glenn St Hilaire[2,3], David Weisz[2,3], Arina D. Omer[2], Melanie Pham[2], Zane Colaric[2], Zhenzhen Yang[9], Suhas S. P. Rao[2,3,10], Namita Mitra[2,3], Christopher Lui[2], Weijie Yao[2], Ruqayya Khan[2,3], Leonid L. Moroz[11], Andrea Kohn[11], Judy St. Leger[12], Alexandria Mena[13], Karen Holcroft[14], Maria Cristina Gambetta[15], Fabian Lim[16], Emma Farley[16], Nils Stein[17,18,19], Alexander Haddad[2], Daniel Chauss[20], Ayse Sena Mutlu[3], Meng C. Wang[3,21,22], Neil D. Young[23], Evin Hildebrandt[24]**, Hans H. Cheng[24], Christopher J. Knight[25], Theresa L. U. Burnham[26,27], Kevin A. Hovel[27], Andrew J. Beel[10], Pierre-Jean Mattei[10], Roger D. Kornberg[10], Wesley C. Warren[28], Gregory Cary[29], José Luis Gómez-Skarmeta[30]††, Veronica Hinman[31], Kerstin Lindblad-Toh[32,33], Federica Di Palma[34], Kazuhiro Maeshima[35,36], Asha S. Multani[37], Sen Pathak[37], Liesl Nel-Themaat[37]‡‡, Richard R. Behringer[37], Parwinder Kaur[19], René H. Medema[5], Bas van Steensel[6], Elzo de Wit[6], José N. Onuchic[4,38], Michele Di Pierro[4,39], Erez Lieberman Aiden[2,3,4,9,19,32]*, Benjamin D. Rowland[1]*

We investigated genome folding across the eukaryotic tree of life. We find two types of three-dimensional (3D) genome architectures at the chromosome scale. Each type appears and disappears repeatedly during eukaryotic evolution. The type of genome architecture that an organism exhibits correlates with the absence of condensin II subunits. Moreover, condensin II depletion converts the architecture of the human genome to a state resembling that seen in organisms such as fungi or mosquitoes. In this state, centromeres cluster together at nucleoli, and heterochromatin domains merge. We propose a physical model in which lengthwise compaction of chromosomes by condensin II during mitosis determines chromosome-scale genome architecture, with effects that are retained during the subsequent interphase. This mechanism likely has been conserved since the last common ancestor of all eukaryotes.

The mechanisms controlling nuclear architecture at the scale of whole chromosomes remain poorly understood. To investigate principles of genome folding, we performed in situ Hi-C (1) on 24 species, representing all subphyla of chordates, all seven extant vertebrate classes, seven of nine major animal phyla, as well as plants and fungi (Fig. 1, figs. S1 and S2, and table S1). For 14 species, there was no existing chromosome-length reference genome assembly.

For these, we upgraded existing genome assemblies or assembled a reference genome entirely from scratch (2) (table S2). Together, these species offer a comprehensive overview of nuclear organization since the last common ancestor of all eukaryotes.

The resulting maps reveal four features of nuclear architecture at the scale of whole chromosomes (Fig. 1 and fig. S1). First, some species, such as the red piranha, exhibit enhanced contact frequency between loci on the same chromosome. This is consistent with, though not necessarily identical to, classical chromosome territories as traditionally observed by cytogenetics—when a chromosome occupies a discrete subvolume of the nucleus, excluding other chromosomes (3). Second, species like the yellow fever and southern domestic mosquitoes exhibit prominent contacts between centromeres. Third, species like the ground peanut exhibit prominent contacts between telomeres. Finally, species like bread wheat exhibit an X-shape on the chromosomal map (Fig. 1 and figs. S1, S2, S3, and S4). We refer to these last three features as Rabl-like, because they are reminiscent of the Rabl chromosome configuration (4), in which centromeres cluster and chromosome arms are arranged in parallel.

To identify these architectural features in an unbiased fashion, we developed aggregate chromosome analysis (ACA), whereby contact maps for each chromosome are rescaled and summed and then used to score each feature (2) (figs. S3 and S6 and table S3). All species that are not holocentric exhibit at least one feature. The architectural features can be divided into two clusters, type-I and type-II, on the basis of how likely the features are to co-occur (fig. S7 and table S4). Type-I includes the three Rabl-like features: centromere clustering, telomere clustering, and a telomere-to-centromere axis. Type-II includes only chromosome territories. Consequently, species can also be subdivided depending on which feature cluster is more strongly exhibited (table S3).

Homologs tend to be separated or paired depending on the species. We found that type-II species typically exhibit homolog separation, whereas this is less frequent among type-I species (figs. S8 and S9 and table S5). We developed an algorithm, dubbed 3D-DNA Phaser, that exploits this separation, when present, to

[1]Division of Gene Regulation, Netherlands Cancer Institute, 1066 CX Amsterdam, Netherlands. [2]The Center for Genome Architecture, Baylor College of Medicine, Houston, TX 77030, USA. [3]Department of Molecular and Human Genetics, Baylor College of Medicine, Houston, TX 77030, USA. [4]Center for Theoretical Biological Physics, Rice University, Houston, TX 77005, USA. [5]Division of Cell Biology, Oncode Institute, Netherlands Cancer Institute, 1066 CX Amsterdam, Netherlands. [6]Division of Gene Regulation, Oncode Institute, Netherlands Cancer Institute, 1066 CX Amsterdam, Netherlands. [7]Department of Physics, Institute of Biosciences, Letters and Exact Sciences, São Paulo State University (UNESP), São José do Rio Preto – SP, 15054-000, Brazil. [8]Biolmaging Facility, Netherlands Cancer Institute, 1066 CX Amsterdam, Netherlands. [9]Shanghai Institute for Advanced Immunochemical Studies, ShanghaiTech, Pudong 201210, China. [10]Department of Structural Biology, Stanford University School of Medicine, Stanford, CA 94305, USA. [11]Whitney Laboratory and Department of Neuroscience, University of Florida, Gainesville, FL 32611, USA. [12]Department of Biosciences, Cornell University College of Veterinary Medicine, Ithaca, NY 14853, USA. [13]SeaWorld San Diego, San Diego, CA 92109, USA. [14]Moody Gardens, Galveston, TX 77554, USA. [15]Center for Integrative Genomics, University of Lausanne, 1015 Lausanne, Switzerland. [16]Department of Medicine and Molecular Biology, University of California, San Diego, La Jolla, CA 92093, USA. [17]Leibniz Institute of Plant Genetics and Crop Plant Research (IPK Gatersleben), 06466 Seeland, Germany. [18]Center of Integrated Breeding Research (CiBreed), Department of Crop Sciences, Georg-August-University Göttingen, 37075 Göttingen, Germany. [19]UWA School of Agriculture and Environment, The University of Western Australia, Perth, WA 6009, Australia. [20]National Institute of Diabetes and Digestive and Kidney Diseases, National Institutes of Health, Bethesda, MD 20892, USA. [21]Huffington Center on Aging, Baylor College of Medicine, Houston, TX 77030, USA. [22]Howard Hughes Medical Institute, Baylor College of Medicine, Houston, TX 77030, USA. [23]Faculty of Veterinary and Agricultural Sciences, University of Melbourne, Parkville, VIC 3010, Australia. [24]Avian Diseases and Oncology Laboratory, US Department of Agriculture, Agricultural Research Service, East Lansing, MI 48823, USA. [25]Hopkins Marine Station, Stanford University, Pacific Grove, CA 93950, USA. [26]Department of Wildlife, Fish, and Conservation Biology, University of California, Davis, Davis, CA 95616, USA. [27]Coastal and Marine Institute and Department of Biology, San Diego State University, San Diego, CA 92106, USA. [28]Department of Animal Sciences, University of Missouri, Columbia, MO 65211, USA. [29]The Jackson Laboratory, Bar Harbor, ME 04609, USA. [30]Centro Andaluz de Biología del Desarrollo CSIC, Universidad Pablo de Olavide, 41013 Sevilla, Spain. [31]Department of Biological Sciences, Carnegie Mellon University, Pittsburgh, PA 15213, USA. [32]Broad Institute of MIT and Harvard, Cambridge, MA 02142, USA. [33]Science for Life Laboratory, Department of Medical Biochemistry and Microbiology, Uppsala University, 751 23 Uppsala, Sweden. [34]Department of Biological Sciences, University of East Anglia, Norwich NR4 7TJ, UK. [35]Genome Dynamics Laboratory, National Institute of Genetics, Mishima, Shizuoka 411-8540, Japan. [36]Department of Genetics, Sokendai (Graduate University for Advanced Studies), Mishima, Shizuoka 411-8540, Japan. [37]Department of Genetics, University of Texas MD Anderson Cancer Center, Houston, TX 77030, USA. [38]Departments of Physics and Astronomy, Chemistry, and Biosciences, Rice University, Houston, TX 77005, USA. [39]Department of Physics, Northeastern University, Boston, MA 02115, USA.

*Corresponding author. Email: b.rowland@nki.nl (B.D.R.); erez@erez.com (E.L.A.)

†These authors contributed equally to this work. ‡Present address: Novartis Institutes for Biomedical Research, 4002 Basel, Switzerland. §These authors contributed equally to this work. ¶Present address: Janssen Vaccines & Prevention BV, 2333 CN Leiden, Netherlands. #Present address: Department of Developmental Biology, Erasmus MC, University Medical Centre Rotterdam, 3015 GD Rotterdam, Netherlands. **Present address: Zoetis (VMRD Global Biologics Research), Kalamazoo, MI 49007, USA. ††Deceased. ‡‡Present address: University of Colorado Advanced Reproductive Medicine, Denver, CO 80238, USA.

assign variants to individual homologs, producing chromosome-length haploblocks for multiple species. When homologs are not separated, as in *Drosophila melanogaster*, we show that this approach cannot be used. Taken together, these data are consistent with a model in which features of genome architecture appeared and disappeared over billions of years, as lineages switched between Rabl-like and territorial architectures.

Next, we sought to understand the mechanism underlying this switching behavior. When investigating the transition between the two architectures, we noted that mosquitoes, which display type-I features (Fig. 1), also lack a
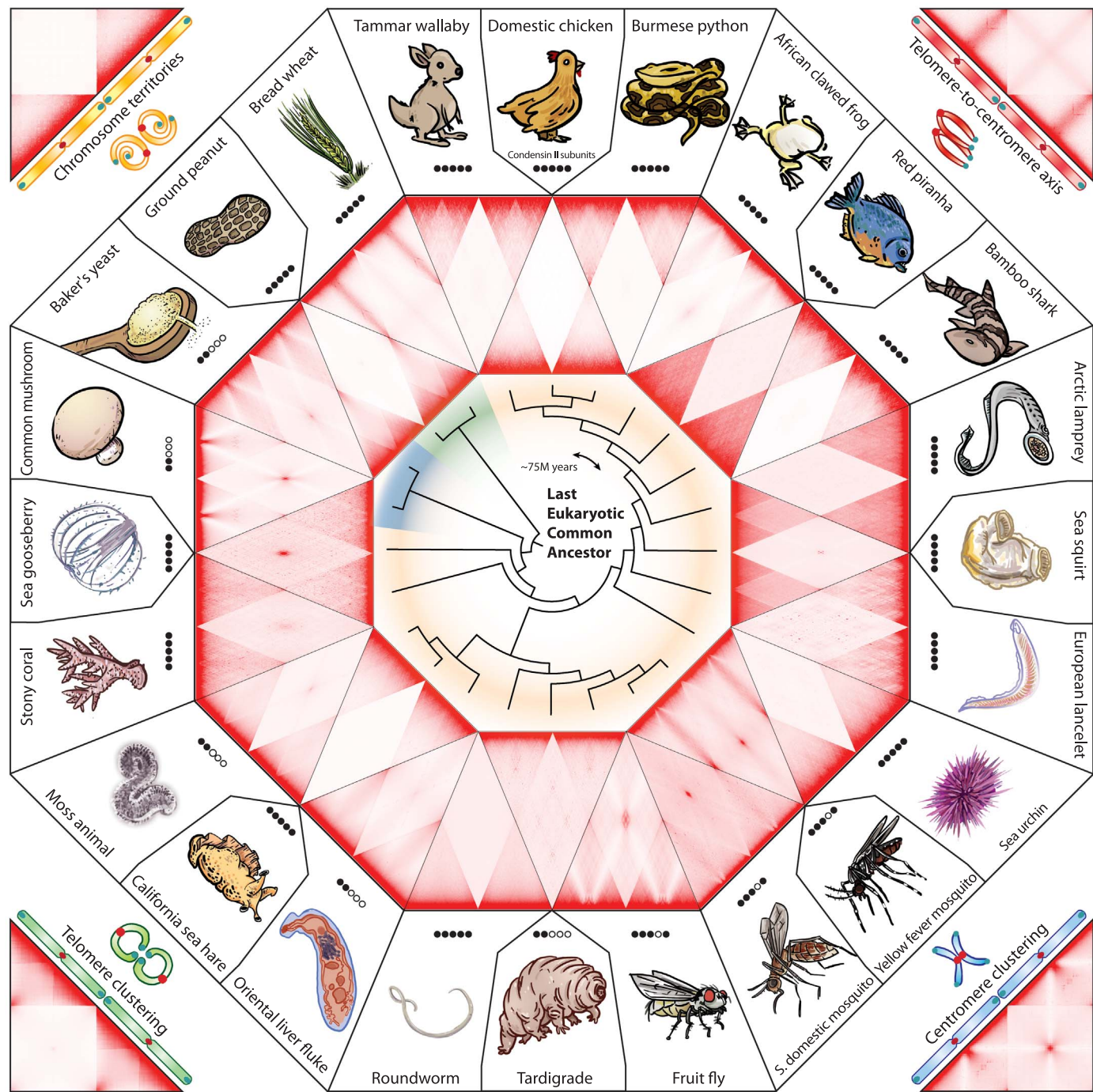
Fig. 1. A comprehensive overview of nuclear architecture across evolution. Aggregate chromosome analysis (ACA) on in situ Hi-C maps of 24 species. In ACA, chromosome arms are rescaled to a uniform length and then the signal of all intra- and interchromosomal contacts is aggregated. This yields an aggregate portrait of genome folding in a species at the scale of whole chromosomes. The 24 ACA plots are rescaled to fit into an octagon, with a depiction of the corresponding species flanking each ACA plot. The species span three kingdoms: animals (yellow), fungi (blue), and plants (green); their evolutionary relationship is represented with a cladogram (2). Each corner shows an example ACA map and a schematic drawing of one of the four chromosome-scale features. The location of these example maps does not correspond to the architecture type of the closest species in the figure. Presence of the condensin II subunits in each species is indicated by solid black circles (left to right: SMC2, SMC4, CAP-H2, CAP-G2, and CAP-D3).
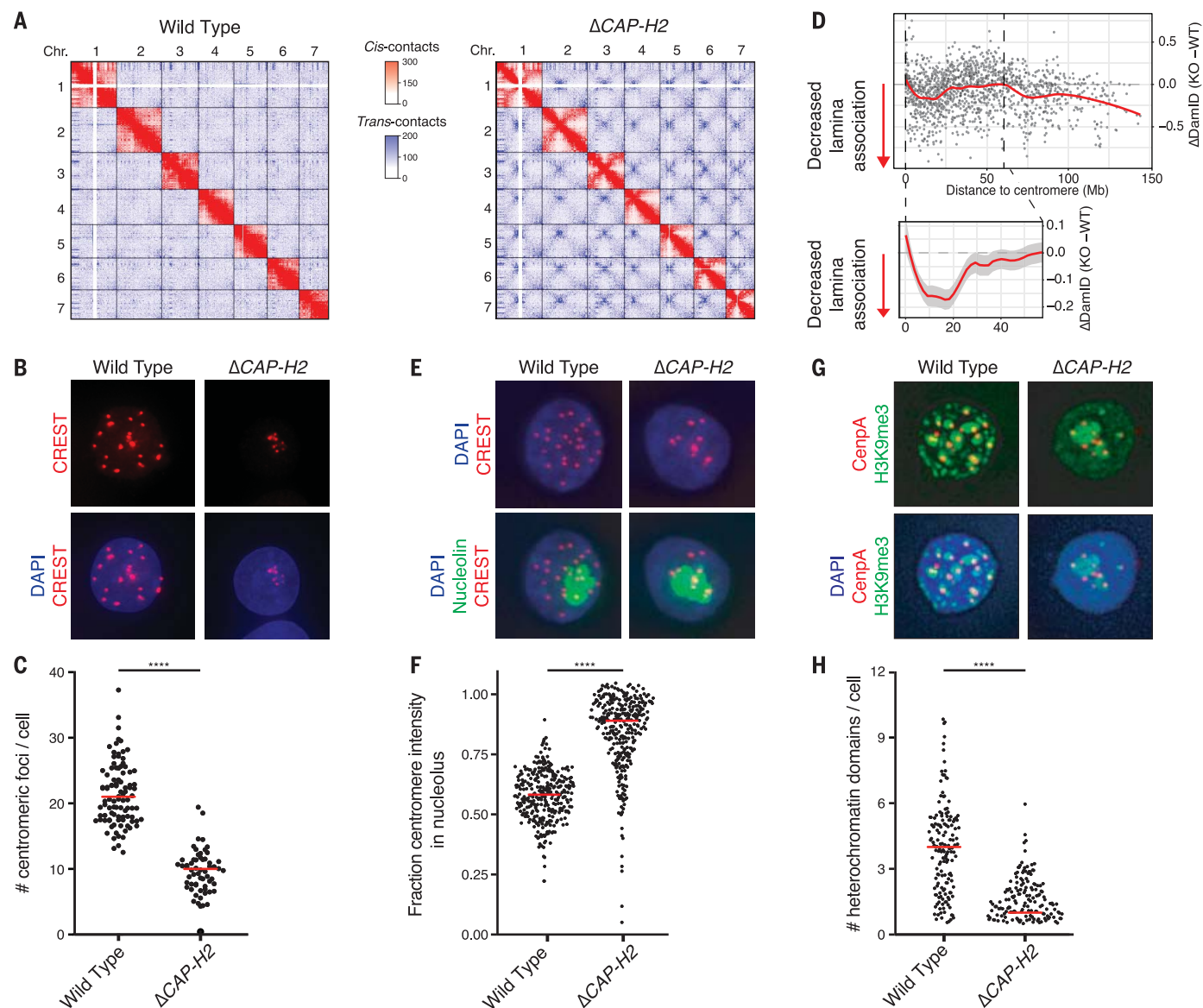
Fig. 2. Condensin II prevents centromeric clustering and keeps apart heterochromatin domains. (**A**) Hi-C matrices of the depicted genotypes in Hap1 cells. Chr., chromosome. (**B** and **C**) Immunofluorescence of centromeres (CREST) and DNA [4',6-diamidino-2-phenylindole (DAPI)] (B), as quantified in (C). (**D**) Difference in DamID score relative to distance to centromere. Zoom-in includes 95% confidence interval of the mean in gray. KO, knockout; WT, wild type. (**E**) Immunofluorescence of centromeres (CREST), nucleoli (nucleolin), and DNA (DAPI). (**F**) Quantification of the fraction of centromere intensity within 0.4 μm of nucleoli, as shown in (E). (**G** and **H**) Immunofluorescence of centromeres (CenpA), heterochromatin (H3K9me3), and DNA (DAPI) (G), as quantified in (H). ****$P < 0.0001$.

subunit of the condensin II complex (5), which promotes mitotic chromosome compaction (6). We therefore searched for condensin II subunits in the genomes of all 24 species. Eight species lacked one or more condensin II subunit(s) (table S6) and exhibited Rabl-like features (table S3). Because these organisms lie far apart on the evolutionary tree, type-I architectural features and the loss of condensin II subunits appear to have coevolved repeatedly. This could indicate that condensin II strengthens chromosome territories or counteracts Rabl-like features.

Notably, of the eight species, five lacked all condensin II subunits, whereas the other three species only lacked CAP-G2. Previous work has shown that condensin complexes lacking the G-subunit still localize to DNA but yield elongated chromosomes (7). Condensin complexes in these species may thus be impaired, at least partially, in their ability to shorten chromosomes.

Humans exhibit type-II genome architecture, with strong chromosomal territories and no Rabl-like features (Fig. 2A). Moreover, human genomes contain all condensin II subunits. Would disruption of condensin II in human cells then interfere with chromosome territories and enhance the strength of type-I features? To test this, we performed in situ Hi-C on Hap1 cells lacking the condensin II subunit CAP-H2 (Fig. 2A, figs. S14 and S15, and table S7). Disruption of this core condensin II subunit prevents recruitment of the CAP-D3 and CAP-G2 subunits to the complex and renders the complex fully nonfunctional.

Δ*CAP-H2* cells exhibited weaker chromosome territories and much stronger contacts between centromeres in trans (Fig. 2A; fig. S15, B and C; and table S8). Immunofluorescence microscopy revealed that in Δ*CAP-H2* cells the centromeres are clustered together. Disruption of condensin II thus transforms the folding of the human genome into a type-I–like configuration (Fig. 2, B and C, and fig. S16).
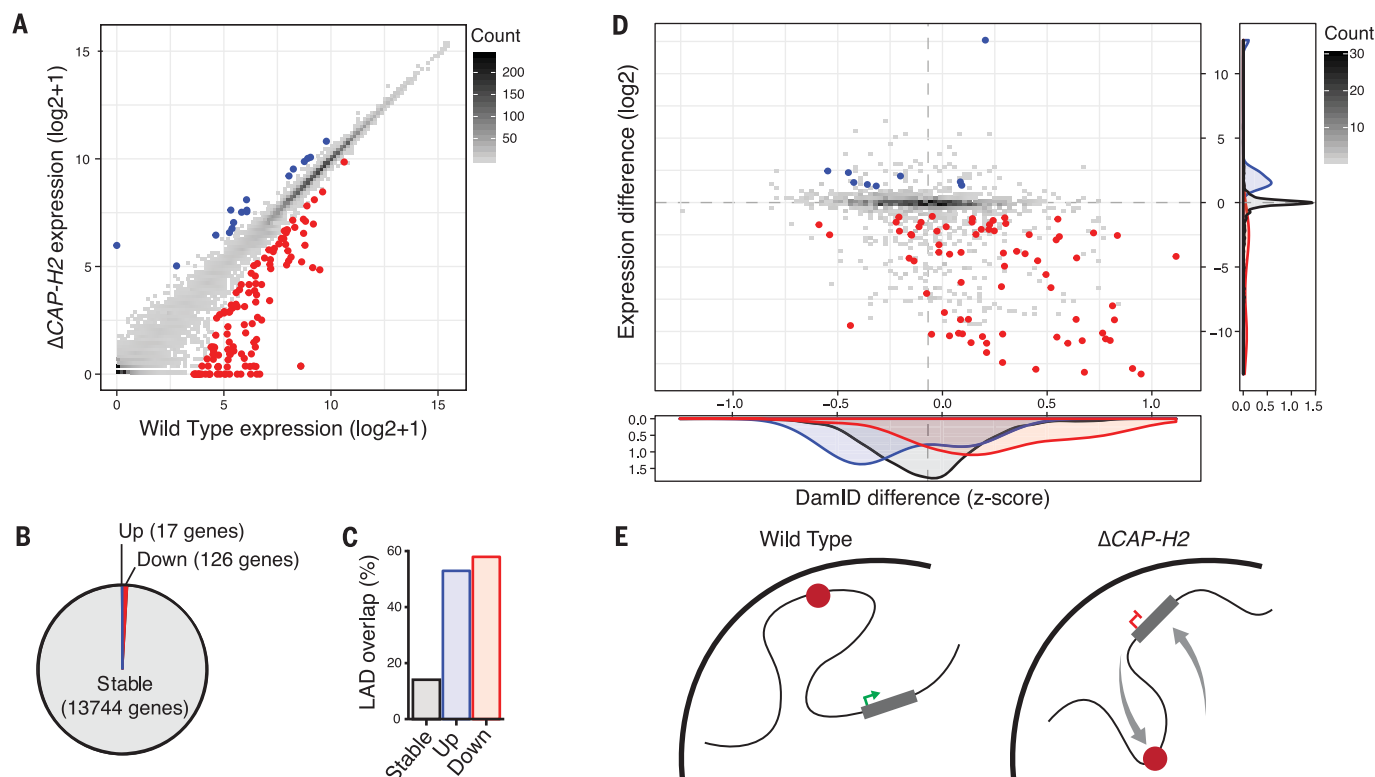
Fig. 3. Massive 3D genome changes hardly affect gene expression.
(**A**) Gene expression of wild type relative to ΔCAP-H2. Unaffected genes are depicted in gray, up-regulated genes in blue, and down-regulated genes in red. (**B**) Number of genes in each category. (**C**) Percentage of active genes overlapping with LADs. (**D**) Intersection of differences in gene expression with differences in lamina association, depicting active genes within LADs. (**E**) Schematic model of centromeres (red) moving to the inner nucleus and silenced genes that now localize to the lamina.

Results previously obtained in other species support the model that condensin II plays a major role in three-dimensional (3D) genome organization. In *Arabidopsis*, condensin II regulates the spatial relationship between ribosomal DNAs (rDNAs) and centromeric regions (*8*, *9*), whereas in mouse cells, condensin II regulates the distribution of chromocenters (*10*). Fruit flies lack a condensin II subunit and exhibit centromeric clustering (Fig. 1). Additional depletion of the remaining condensin II subunits in flies affects the spatial distribution of pericentromeric heterochromatin and leads to intermixing of chromosome territories, further strengthening the existing Rabl-like features (*11*, *12*).

Next, we investigated the effects of condensin II loss on human genome architecture in greater detail. To identify DNA segments associated with the nuclear lamina [lamina-associated domains (LADs)], we performed DamID of LaminB1 (*13*) (fig. S17A). LADs localizing up to 25 Mb from the centromeres appeared to move away from the lamina (Fig. 2D and fig. S17, B and C). Centromere repositioning in absence of condensin II thus also moderately affects the lamina association of the regions flanking the centromeres.

In fruit flies, centromeres cluster and localize to the nucleolus (*14*). In ΔCAP-H2 human cells, centromeres also cluster in or around the nucleolus (Fig. 2, E and F). However, disrupting nucleolar structure did not affect centromeric clustering (fig. S18, A and B). The clustering of centromeres at the human nucleolus is likely because rDNA sequences, which are the genomic component of the nucleolus, often lie near centromeres in the human genome (on the short arm of acrocentric chromosomes) (fig. S18C).

Regions surrounding centromeres are enriched for heterochromatin and cluster upon condensin II depletion in mice and fruit flies (*10*, *11*). Similarly, in ΔCAP-H2 cells, condensin II deficiency led to clustering of H3K9me3-containing heterochromatin (Fig. 2, G and H), which indicates that condensin II plays a conserved role in the spatial organization of this repressive epigenetic mark. Condensin II deficiency did not affect smaller-scale 3D genome organization at the level of chromatin loops (fig. S19, A and B). Also, compartmentalization was only mildly affected, specifically in regions surrounding the centromeres (fig. S19, C and D). Thus, large-scale reorganization does not necessarily bring about major changes in smaller-scale structures.

RNA sequencing revealed that condensin II deficiency affected the expression of only a fraction of genes (Fig. 3, A and B), which were enriched within LADs (Fig. 3C) and near LAD borders (fig. S20, B and C). The down-regulated genes moved toward the lamina (Fig. 3D). Genes that are near or within LADs could potentially occupy the space that is vacated by the centromeres moving to the nuclear interior upon condensin II loss. The increased lamina association of these genes may, in turn, lead to their transcriptional repression, although the gain in lamina interactions could also be the consequence of the reduced expression of these genes (*15*, *16*) (Fig. 3E).

Thus, condensin II controls the architecture of the interphase genome, but whether it does so by acting in interphase remained unclear. We therefore acutely depleted condensin II in HCT116 cells (*17*) at the G$_1$-S cell cycle phase transition and either halted the cells before mitotic entry or allowed the cells to progress through mitosis (Fig. 4, A and B, and fig. S21A). When condensin II–depleted cells were halted before mitosis, centromeres did not cluster, which is consistent with condensin II depletion in postmitotic cells not changing the 3D genome (*18*). By contrast, progression through mitosis led to clear centromeric clustering in the subsequent G$_1$ phase. This suggests that condensin II acts in mitosis, or directly

thereafter, to establish 3D genome organization for the next interphase (fig. S21B).

In mitosis, condensin II extrudes loops to compact chromosomes in a lengthwise manner (19–21). We used physical simulations to investigate whether this activity of condensin II can affect centromere clustering. In these simulations, chromosomes are polymers bisected by a centromere. These chromosomes are shaped by two forces: (i) the ideal chromosome potential that models lengthwise compaction by condensin II (22, 23) and (ii) centromeric self-adhesion, which models heterochromatin's tendency to cluster (24–26) and stabilizes intercentromeric contacts in our setup. We simulated 10 chromosomes with fixed centromere self-adhesion and decreased lengthwise compaction to model condensin II depletion (Fig. 4, C to G; fig. S22; and table S9).

Under high lengthwise compaction (i.e., intact condensin II), chromosomes form non-overlapping entities and hinder the spatial clustering of centromeres. Correspondingly, lower lengthwise compaction (i.e., impaired condensin II) leads to chromosome intermingling and centromere clustering. This physical model illustrates how the loss of lengthwise compaction might explain the observed clustering of centromeres.

Condensin I and condensin II together drive mitotic chromosome condensation (fig. S23, A and B). In contrast to condensin II, condensin I primarily decreases the width of the chromosome (19, 20). If condensin II–driven lengthwise compaction were the key factor leading to territorialization, rather than chromosome
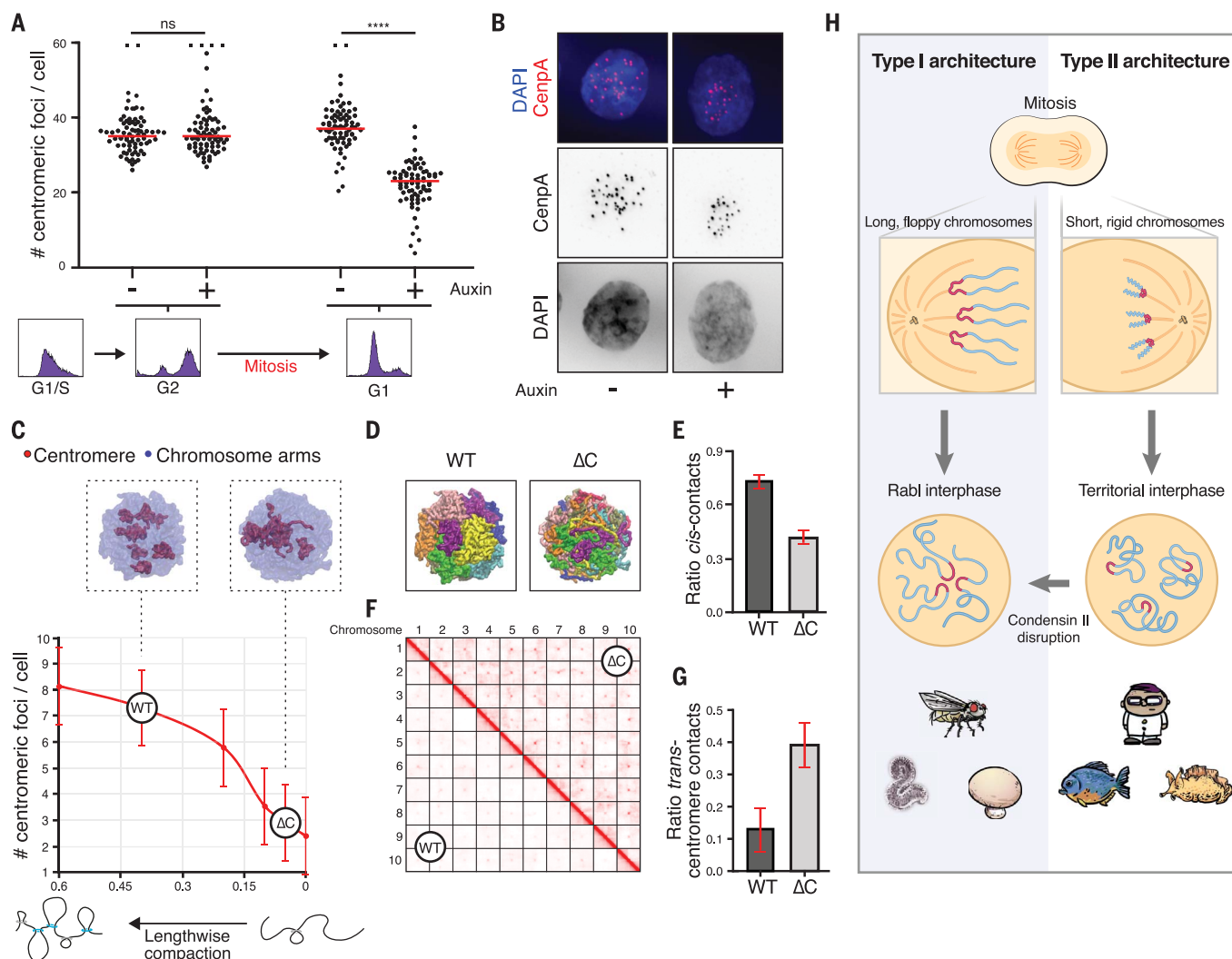
Fig. 4. Centromeric clustering is counteracted by lengthwise compaction and requires mitosis-to-interphase transition. (**A**) Quantification of centromeric foci before or after mitotic progression with or without auxin-mediated condensin II degradation. Fluorescence-activated cell sorting (FACS) plots depict cell cycle stages. Outliers (>60) were truncated and depicted as squares. (**B**) Example images of G_1 cells as quantified in (A). (C to G) Simulation modeling using ten polymer chains as chromosomes. (**C**) Number of centromere clusters upon varying lengthwise compaction (strength of the ideal chromosome term). WT and ΔC correspond to higher and lower lengthwise compaction, recapitulating the experimental data observed in wild type and ΔCAP-H2 cells. (Top) Representative models for both states.

(**D**) Representative simulation snapshots depicting ten chromosomes in different colors. (**E**) Quantification of the ratio of cis contacts. (**F**) Simulated Hi-C matrices depicting contacts between the respective chromosomes. (**G**) Quantification of the proportion of trans-centromeric contacts. (**H**) Model for the establishment of type-I and type-II genome architectures. Having shorter chromosomes during mitosis tends to interfere with adhesion between centromeres, leading to separate centromeres and territorial genome architecture in the subsequent interphase. Reducing lengthwise compaction, for example by condensin II disruption, leads to enhanced centromere clustering, loss of chromosome territories, and a Rabl-like genome architecture. ****$P < 0.0001$; ns, not significant.

condensation in general, then condensin I depletion would not lead to a shift from territorial to Rabl-like architecture. We found that acute depletion of the condensin I subunit CAP-H did not lead to centromeric clustering (fig. S23, C and D).

Evolution has performed an experiment in which chromosome length varies as a result of chromosome fusions rather than the loss of condensin II. Specifically, the Chinese muntjac has 46 short chromosomes that have merged, in the closely related Indian muntjac, into six chromosomes (in females). By assembling the muntjac genomes, we found that the notable increase in chromosome length in the Indian muntjac coincides, as expected, with the appearance of centromeric clustering (fig. S25).

Taken together, a model emerges in which condensin II establishes interphase 3D genome architecture at the scale of whole chromosomes. We hypothesize that (i) centromeres tend to adhere to one another, a process that is facilitated by proximity during and shortly after mitosis; (ii) the shortening of chromosomes interferes with this adhesion, enabling the centromeres to spread out over the newly formed nuclei; and (iii) chromosome territories emerge as a by-product of the resulting chromosomal separation (Fig. 4H).

The role of condensin II in establishing the overall architecture of the genome appears to be among the most ancient capabilities defining genome folding in the eukaryotic lineage. Changes in condensin II have likely contributed to notable shifts from chromosome territories to Rabl-like features throughout the tree of life. As our exploration of the tree of life continues, one of the many fruits will be a deeper knowledge of our own cellular machinery.

REFERENCES AND NOTES

1. S. S. P. Rao et al., Cell 159, 1665–1680 (2014).
2. Materials and methods are available as supplementary materials online.
3. T. Cremer, M. Cremer, Cold Spring Harb. Perspect. Biol. 2, a003889 (2010).
4. C. Rabl, Morphol. Jahrb. 10, 214–330 (1885).
5. T. D. King et al., Mol. Biol. Evol. 36, 2195–2204 (2019).
6. T. Hirano, Cell 164, 847–857 (2016).
7. K. Kinoshita, T. J. Kobayashi, T. Hirano, Dev. Cell 33, 94–106 (2015).
8. V. Schubert, I. Lermontova, I. Schubert, Chromosoma 122, 517–533 (2013).
9. T. Sakamoto, T. Sugiyama, T. Yamashita, S. Matsunaga, Nucleus 10, 116–125 (2019).
10. K. Nishide, T. Hirano, PLOS Genet. 10, e1004847 (2014).
11. C. R. Bauer, T. A. Hartl, G. Bosco, PLOS Genet. 8, e1002873 (2012).
12. L. F. Rosin, S. C. Nguyen, E. F. Joyce, PLOS Genet. 14, e1007393 (2018).
13. L. Guelen et al., Nature 453, 948–951 (2008).
14. J. Padeken et al., Mol. Cell 50, 236–249 (2013).
15. L. Brueckner et al., EMBO J. 39, e103159 (2020).
16. B. van Steensel, A. S. Belmont, Cell 169, 780–791 (2017).
17. M. Takagi et al., J. Cell Sci. 131, jcs212092 (2018).
18. N. Abdennur et al., Condensin II inactivation in interphase does not affect chromatin folding or gene expression. bioRxiv 437459 [Preprint]. 7 October 2018. https://doi.org/10.1101/437459.
19. K. Shintomi, T. Hirano, Genes Dev. 25, 1464–1469 (2011).
20. L. C. Green et al., J. Cell Sci. 125, 1591–1604 (2012).
21. J. H. Gibcus et al., Science 359, eaao6135 (2018).
22. B. Zhang, P. G. Wolynes, Phys. Rev. Lett. 116, 248101 (2016).
23. M. Di Pierro, B. Zhang, E. L. Aiden, P. G. Wolynes, J. N. Onuchic, Proc. Natl. Acad. Sci. U.S.A. 113, 12168–12173 (2016).
24. A. G. Larson et al., Nature 547, 236–240 (2017).
25. A. R. Strom et al., Nature 547, 241–245 (2017).
26. M. Falk et al., Nature 570, 395–399 (2019).
27. C. Hoencamp, Data from: 3D genomics across the tree of life identifies condensin II as a determinant of architecture type, version 1, Harvard Dataverse (2021); https://doi.org/10.7910/DVN/UROKAG.
28. O. Dudchenko, E. Lieberman-Aiden, S. Singh Batra, aidenlab/3d-dna: 3D-DNA Phasing branch 201008, version 201008, Zenodo (2021); http://doi.org/10.5281/zenodo.4619943.
29. T. van den Brand, R. van der Weide, A. Sedeño Cacciatore, M. Schijns, deWitLab/GENOVA v0.94, version v0.94, Zenodo (2021); http://doi.org/10.5281/zenodo.4564568.
30. Á. Sedeño Cacciatore, asedenocacciatore/centromeric_clustering: v0.1, version v0.1, Zenodo (2021); http://doi.org/10.5281/zenodo.4575422.
31. C. Hoencamp et al., 3D genomics across the tree of life reveals condensin II as a determinant of architecture type, dataset, Zenodo (2021); http://doi.org/10.5281/zenodo.4582361.
32. O. Dudchenko, duddcha/misc: Analysis of heritability of architectural features, custom script, version Hoencamp, Zenodo (2021); http://doi.org/10.5281/zenodo.4619996.
33. B. van den Broek, bvandenbroek/intensity-distribution-nucleoli: Version 1.0.0, version 1.0.0, Zenodo (2020); http://doi.org/10.5281/zenodo.4350575.

Science

3D genomics across the tree of life reveals condensin II as a determinant of architecture type

Claire HoencampOlga DudchenkoAhmed M. O. ElbatshSumitabha BrahmachariJonne A. RaaijmakersTom van SchaikÁngela Sedeño CacciatoreVinícius G. ContessotoRoy G. H. P. van HeesbeenBram van den BroekAditya N. MhaskarHans TeunissenBrian Glenn St HilaireDavid WeiszArina D. OmerMelanie PhamZane ColaricZhenzhen YangSuhas S. P. RaoNamita MitraChristopher LuiWeijie YaoRuqayya KhanLeonid L. MorozAndrea KohnJudy St. LegerAlexandria MenaKaren HolcroftMaria Cristina GambettaFabian LimEmma FarleyNils SteinAlexander HaddadDaniel ChaussAyse Sena MutluMeng C. WangNeil D. YoungEvin HildebrandtHans H. ChengChristopher J. KnightTheresa L. U. BurnhamKevin A. HovelAndrew J. BeelPierre-Jean MatteiRoger D. KornbergWesley C. WarrenGregory CaryJosé Luis Gómez-SkarmetaVeronica HinmanKerstin Lindblad-TohFederica Di PalmaKazuhiro MaeshimaAsha S. MultaniSen PathakLiesl Nel-ThemaatRichard R. BehringerParwinder KaurRené H. MedemaBas van SteenselElzo de WitJosé N. OnuchicMichele Di PierroErez Lieberman AidenBenjamin D. Rowland

Organismal evolution of the 3D genome

The conformation of chromosomes within the nucleus can reflect a cell's type or state. However, studies of the conservation and evolutionary history of the mechanisms regulating genome structure across species are lacking. Hoencamp *et al.* mapped three-dimensional (3D) genome organization in 24 eukaryote species, including animals, fungi, and plants. At interphase, species' telomeres and centromeres either clustered across chromosomes or oriented in a polarized state maintaining individual chromosomal territories within the cell, a difference attributed to condensin II. An experimental loss of condensin II in human cells promotes the formation of centromere clusters but has no effect on loop or compartment formation. Whether the structure of the 3D genome varies across species may thus depend on whether they carry a functional condensin II gene.

View the article online
https://www.science.org/doi/10.1126/science.abe2218
Permissions
https://www.science.org/help/reprints-and-permissions

Use of think article is subject to the Terms of service